Research Article | Vol. 26, No. 3 | 5 Feb 2018 | OPTICS EXPRESS 2341

Optics EXPRESS

Microwave spectroscopy measurement of ultracold ground state molecules produced via short-range photoassociation

ZHONGHAO LI,[1,2] ZHONGHUA JI,[1,2] TING GONG,[1,2] JUANJUAN CAO,[1,2] YANTING ZHAO,[1,2,*] LIANTUAN XIAO,[1,2] AND SUOTANG JIA[1,2]

[1]*State Key Laboratory of Quantum Optics and Quantum Optics Devices, Institute of Laser Spectroscopy, Shanxi University, Taiyuan 030006, China*
[2]*Collaborative Innovation Center of Extreme Optics, Shanxi University, Taiyuan 030006, China*
[*]*zhaoyt@sxu.edu.cn*

Abstract: The high-resolution microwave (MW) spectroscopy is employed to measure the rotational structures of ultracold $^{85}Rb^{133}Cs$ molecules prepared in the $X^1\Sigma^+$ (v = 0) ground state. These ground-state molecules are created using short-range photoassociation (PA) followed by the spontaneous emission. Using a combination of continuous-wave (CW) depletion spectroscopy and photoionization (PI) technique, we obtain the MW spectroscopy by coupling the neighboring rotational levels of ground-state molecules. Based on the frequency spacing obtained from the MW spectroscopy, the rotational constant of $X^1\Sigma^+$ (v = 0) can be accurately determined with the rigid rotor model. The precision of the measurement by MW spectroscopy is found to be 3 orders of magnitude higher than the CW depletion spectroscopy. Our scheme provides a simple and highly accurate method for the measurement of molecular structure.

© 2018 Optical Society of America under the terms of the OSA Open Access Publishing Agreement

OCIS codes: (020.3320) Laser cooling; (300.6320) Spectroscopy, high-resolution; (300.6370) Spectroscopy, microwave; (300.6390) Spectroscopy, molecular.

References and links

1. T. Zelevinsky, S. Kotochigova, and J. Ye, "Precision test of mass-ratio variations with lattice-confined ultracold molecules," Phys. Rev. Lett. **100**(4), 043201 (2008).
2. S. Schiller, "Hydrogenlike highly charged ions for tests of the time independence of fundamental constants," Phys. Rev. Lett. **98**(18), 180801 (2007).
3. D. DeMille, S. B. Cahn, D. Murphree, D. A. Rahmlow, and M. G. Kozlov, "Using molecules to measure nuclear spin-dependent parity violation," Phys. Rev. Lett. **100**(2), 023003 (2008).
4. J. Rui, H. Yang, L. Liu, D. Zhang, Y. Liu, J. Nan, Y. Chen, B. Zhao, and J. Pan, "Controlled state-to-state atom-exchange reaction in an ultracold atom–dimer mixture," Nat. Phys. **13**(7), 699–703 (2017).
5. S. Ospelkaus, K.-K. Ni, D. Wang, M. H. G. de Miranda, B. Neyenhuis, G. Quéméner, P. S. Julienne, J. L. Bohn, D. S. Jin, and J. Ye, "Quantum-state controlled chemical reactions of ultracold potassium-rubidium molecules," Science **327**(5967), 853–857 (2010).
6. D. DeMille, "Quantum computation with trapped polar molecules," Phys. Rev. Lett. **88**(6), 067901 (2002).
7. C. Chin, R. Grimm, P. Julienne, and E. Tiesinga, "Feshbach resonances in ultracold gases," Rev. Mod. Phys. **82**(2), 1225–1286 (2010).
8. J. Ulmanis, J. Deiglmayr, M. Repp, R. Wester, and M. Weidemüller, "Ultracold molecules formed by photoassociation: heteronuclear dimers, inelastic collisions, and interactions with ultrashort laser pulses," Chem. Rev. **112**(9), 4890–4927 (2012).
9. C. R. Menegatti, B. S. Marangoni, N. Bouloufa-Maafa, O. Dulieu, and L. G. Marcassa, "Trap loss in a rubidium crossed dipole trap by short-range photoassociation," Phys. Rev. A **87**(5), 053404 (2013).
10. M. A. Bellos, D. Rahmlow, R. Carollo, J. Banerjee, O. Dulieu, A. Gerdes, E. E. Eyler, P. L. Gould, and W. C. Stwalley, "Formation of ultracold Rb_2 molecules in the $v'' = 0$ level of the $a^3\Sigma^+_u$ state via blue-detuned photoassociation to the $1^3\Pi_g$ state," Phys. Chem. Chem. Phys. **13**(42), 18880–18886 (2011).
11. J. Deiglmayr, A. Grochola, M. Repp, K. Mörtlbauer, C. Glück, J. Lange, O. Dulieu, R. Wester, and M. Weidemüller, "Formation of ultracold polar molecules in the rovibrational ground state," Phys. Rev. Lett. **101**(13), 133004 (2008).
12. J. Banerjee, D. Rahmlow, R. Carollo, M. Bellos, E. E. Eyler, P. L. Gould, and W. C. Stwalley, "Direct photoassociative formation of ultracold KRb molecules in the lowest vibrational levels of the electronic ground state," Phys. Rev. A **86**(5), 053428 (2012).

#310086 https://doi.org/10.1364/OE.26.002341
Journal © 2018 Received 26 Oct 2017; revised 11 Jan 2018; accepted 18 Jan 2018; published 23 Jan 2018

Optics EXPRESS

13. P. Zabawa, A. Wakim, M. Haruza, and N. P. Bigelow, "Formation of ultracold $X^1\Sigma^+$ (v" = 0) NaCs molecules via coupled photoassociation channels," Phys. Rev. A **84**(6), 061401 (2011).
14. C. Gabbanini and O. Dulieu, "Formation of ultracold metastable RbCs molecules by short-range photoassociation," Phys. Chem. Chem. Phys. **13**(42), 18905–18909 (2011).
15. N. Bouloufa-Maafa, M. Aymar, O. Dulieu, and C. Gabbanini, "Formation of ultracold RbCs molecules by photoassociation," Laser Phys. **22**(10), 1502–1512 (2012).
16. Z. Ji, H. Zhang, J. Wu, J. Yuan, Y. Yang, Y. Zhao, J. Ma, L. Wang, L. Xiao, and S. Jia, "Photoassociative formation of ultracold RbCs molecules in the $(2)^3\Pi$ state," Phys. Rev. A **85**(1), 013401 (2012).
17. A. Fioretti and C. Gabbanini, "Experimental study of the formation of ultracold RbCs molecules by short-range photoassociation," Phys. Rev. A **87**(5), 054701 (2013).
18. C. D. Bruzewicz, M. Gustavsson, T. Shimasaki, and D. DeMille, "Continuous formation of vibronic ground state RbCs molecules via photoassociation," New J. Phys. **16**(2), 023018 (2014).
19. D. B. Blasing, I. C. Stevenson, J. Pérez-Ríos, D. S. Elliott, and Y. P. Chen, "Short-range photoassociation of LiRb," Phys. Rev. A **94**(6), 062504 (2016).
20. D. Wang, J. T. Kim, C. Ashbaugh, E. E. Eyler, P. L. Gould, and W. C. Stwalley, "Rotationally resolved depletion spectroscopy of ultracold KRb molecules," Phys. Rev. A **75**(3), 032511 (2007).
21. K. Aikawa, D. Akamatsu, J. Kobayashi, M. Ueda, T. Kishimoto, and S. Inouye, "Toward the production of quantum degenerate bosonic polar molecules, $^{41}K^{87}Rb$," New J. Phys. **11**(5), 055035 (2009).
22. T. Shimasaki, M. Bellos, C. D. Bruzewicz, Z. Lasner, and D. DeMille, "Production of rovibronic-ground-state RbCs molecules via two-photon-cascade decay," Phys. Rev. A **91**(2), 021401 (2015).
23. I. C. Stevenson, D. B. Blasing, Y. P. Chen, and D. S. Elliott, "Production of ultracold ground-state LiRb molecules by photoassociation through a resonantly coupled state," Phys. Rev. A **94**(6), 062510 (2016).
24. Z. Ji, Z. Li, T. Gong, Y. Zhao, L. Xiao, and S. Jia, "Rotational population measurement of ultracold ^{85}Rb ^{133}Cs molecules in the lowest vibrational ground state," Chin. Phys. Lett. **34**(10), 103301 (2017).
25. J. Yuan, Y. Zhao, Z. Ji, Z. Li, J. T. Kim, L. Xiao, and S. Jia, "The determination of potential energy curve and dipole moment of the $(5)0^+$ electronic state of $^{85}Rb^{133}Cs$ molecule by high resolution photoassociation spectroscopy," J. Chem. Phys. **143**(22), 224312 (2015).
26. W. Ketterle, K. B. Davis, M. A. Joffe, A. Martin, and D. E. Pritchard, "High densities of cold atoms in a dark spontaneous-force optical trap," Phys. Rev. Lett. **70**(15), 2253–2256 (1993).
27. A. R. Allouche, M. Korek, K. Fakherddin, A. Chaalan, M. Dagher, F. Taher, and M. Aubert-Frécon, "Theoretical electronic structure of RbCs revisited," J. Phys. At. Mol. Opt. Phys. **33**(12), 2307–2316 (2000).
28. H. Fahs, A. R. Allouche, M. Korek, and M. Aubert-Frécon, "The theoretical spin–orbit structure of the RbCs molecule," J. Phys. At. Mol. Opt. Phys. **35**(6), 1501–1508 (2002).
29. Z. Ji, J. Yuan, Y. Yang, Y. Zhao, L. Xiao, and S. Jia, "Photoionization spectrum of $^{85}RbCs$ molecules produced by short range photoassociation," J. Quant. Spectrosc. Radiat. Transf. **166**, 36–41 (2015).
30. Y. Lee, Y. Yoon, S. Lee, J. T. Kim, and B. Kim, "Parallel and coupled perpendicular transitions of RbCs 640 nm system: Mass-resolved resonance enhanced two-photon ionization in a cold molecular beam," J. Phys. Chem. A **112**(31), 7214–7221 (2008).
31. J. Aldegunde, B. A. Rivington, P. S. Żuchowski, and J. M. Hutson, "Hyperfine energy levels of alkali-metal dimers: Ground-state polar molecules in electric and magnetic fields," Phys. Rev. A **78**(3), 033434 (2008).
32. M. Lysebo and L. Veseth, "Cold collisions between atoms and diatomic molecules," Phys. Rev. A **77**(3), 032721 (2008).
33. C. E. Fellows, R. F. Gutterres, A. P. Campos, J. Vergès, and C. Amiot, "The RbCs $X^1\Sigma^+$ ground electronic state: New spectroscopic study," J. Mol. Spectrosc. **197**(1), 19–27 (1999).

1. Introduction

The preparation and manipulation of ultracold ground-state molecules produced from ultracold atoms have attracted intensive attention in the past few years. Benefiting from the rich internal structure and inter-molecular interactions, ultracold molecules have opened new possibilities for precision measurement [1–3], quantum control of cold chemical reactions [4,5], and quantum computation [6]. The approach to create ultracold ground-state molecules mainly includes magnetically tunable Feshbach resonance [7] and photoassociation (PA) [8]. In this context, the PA (in particular short-range PA) is widely used for its simplicity and convenience, as has been demonstrated in Rb_2 [9,10], $^7Li^{133}Cs$ [11], $^{39}K^{85}Rb$ [12], $^{23}Na^{133}Cs$ [13], $^{85}Rb^{133}Cs$ [14–18], $^7Li^{85}Rb$ [19] *et al.*.

The accurate structural information about the ultracold ground-state molecules allows determination of molecular structure constants, the detailed description of electronic character of molecular bonds, the manipulation of molecular states, and the investigation of molecular state chemistry. In order to obtain the structural information of ground-state molecules produced by short-range PA, the photoionization (PI) combined with time-of-flight (TOF) mass spectrometry [10–19] is usually adopted with vibrational selectivity. However, the

Optics EXPRESS

linewidth of the pulsed lasers used for ionization is usually larger than the energy spacing between rotational levels. Therefore, it is impossible to distinguish single rotational level and the rotational structural information. To solve this problem, the rotational level identification has been achieved by way of continuous-wave (CW) depletion spectroscopy [11,13,20–24]. Using a narrow linewidth (~MHz) CW laser, the rotational population for the molecules in one vibrational state can be determined. Specifically, considering the linewidth of the depletion spectroscopy is ~100MHz, and taking into account of the molecular structure of excited state, the uncertainty of structural information obtained from depletion spectroscopy is estimated as ~10MHz [11,20,23,24].

We note that the frequency spacing between the rotational levels is within the microwave (MW) region. In addition, the rotational degrees of freedom of molecules allow a set of excited rotational states which can be easily coupled to the ground state using the MW field. Thus, the MW spectroscopy of transitions between rotational levels presents an ideal tool for probing the rotational structure. In particular, the rotational levels could be coupled directly via MW, such that the correction from molecular structure in the excited states can be ignored in contrast to CW depletion. As a result, the rotational structural information via MW spectroscopy with narrow intrinsic linewidth allows achievement of higher precision.

In this paper, the high-resolution MW spectroscopy is employed to detect the structural information of ultracold $^{85}Rb^{133}Cs$ molecules in the $X^1\Sigma^+$ (v = 0) ground state realized via short-range PA. Basing on the electric-dipole allowed rotational transitions, we use the MW field to couple the neighboring rotational levels directly. The MW spectroscopy can be obtained as a result of combinations of the CW depletion spectroscopy and PI technique. The neighboring rotational frequency spacing is determined using the depletion and MW spectroscopy. The obtained frequency spacing is fitted with a rigid rotor model to determine the rotational constant for $^{85}Rb^{133}Cs$ molecules in the $X^1\Sigma^+$ (v = 0) state.

2. Experimental setup

Most details of the apparatus have been described before [24,25]. Our experiment starts with a mixed ^{85}Rb-^{133}Cs cold sample prepared in the dark spontaneous force optical traps (dark-SPOTs) [26]. Under a vacuum background pressure of around 3×10^{-7} Pa and a magnetic gradient of around 15 G/cm, we trap a mixed atomic cloud which consists of ~1×10^7 ^{85}Rb atoms in the $5S_{1/2}$ (F = 2) state and ~2×10^7 ^{133}Cs atoms in the $6S_{1/2}$ (F = 3) state. The atomic density of ^{85}Rb atoms is 8×10^{10} cm^{-3}, and that of ^{133}Cs atoms is 1×10^{11} cm^{-3}. The translational temperature of the mixed atoms is measured to be around 100 μK by way of TOF imaging.

Figure 1(a) illustrates the formation and detection mechanisms of ultracold $^{85}Rb^{133}Cs$ molecules in the $X^1\Sigma^+$ (v = 0) ground state. To form the $^{85}Rb^{133}Cs$ molecules in the $X^1\Sigma^+$ (v = 0) state, the cold mixed atomic sample is irradiated by the PA laser, which is generated by employing a tunable Ti: sapphire laser system with a typical linewidth of 100 kHz and an output power of up to 1.5 W. We focus the PA beam on the center of the overlapped dark-SPOTs with the Gaussian radius of 150 μm. The PA laser is locked by a subtle transfer cavity technique [29] to the selected rotational level (J = 0 or J = 1) of $2^3\Pi_0$ + (v = 10) at a short range. The uncertainty of locked PA laser frequency can be less than 2 MHz. The molecules in the vibrational ground state $X^1\Sigma^+$ (v = 0) are formed via two-photon-cascade decay [22]. The molecules in $X^1\Sigma^+$ (v = 0) are ionized by a tunable pulsed dye laser through the one-color resonance-enhanced two-photon ionization (RETPI) [24]. The pulse energy is about 2mJ with a diameter of about 3mm and the pulse width is 7ns. Since the linewidth of the dye laser (~6 GHz) is larger than the energy spacing between rotational levels, it is impossible to address molecules in a single rotational level.

To deplete the population of any given rotational level in the $X^1\Sigma^+$ (v = 0) state, an additional CW diode laser is used. We choose the $2^3\Pi_0$ + (v = 8) level as the upper state of this depletion transition, whose molecular constant is well known [25,30]. The depletion

Optics EXPRESS

laser, locked by the transfer cavity technique as well, is obtained by a homemade external cavity diode laser with a power of ~7 mW and a diameter of ~1 mm. Since the PA and depletion laser share the same reference cavity, the uncertainty of the locked depletion laser frequency can also be less than 2 MHz.

(a)

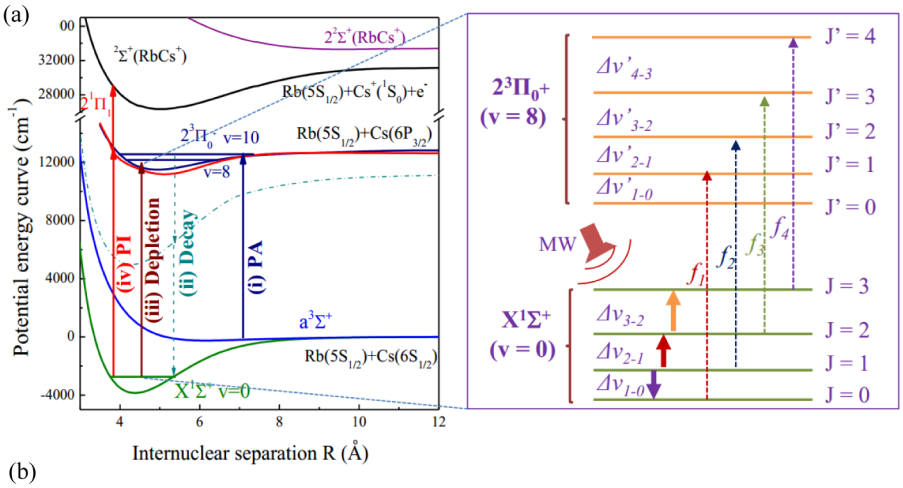

(b)

	Dark-SPOTs (90ms)	Transition & depletion (2ms)	Detection (8ms)
Cooling &PA lasers			
Magnetic field			
MW			
Depletion laser			
PI laser			7ns
Electric field			20μs

Fig. 1. (a) Formation and detection mechanism for ultracold $^{85}Rb^{133}Cs$ molecules in the $X^1\Sigma^+$ (v = 0) state. The potential energy curves are based on the data [27,28]. The partial enlarged detail shows the related energy levels in the measurement of depletion and MW spectroscopy. (b) The time sequence in our experiment. The shadow with different color means "on", the blank means "off", and the "oblique line" means the MW can be "selectively on or off" for different measurement.

The MW field is supported by a RF signal generator (Stanford Research Systems, SG386), as referenced to a rubidium time-base. A fast (~ns) switch is used to generate MW pulses with well-defined duration. After a power amplifier (Mini-Circuits, ZHL-4W-422 +), the MW field is radiated on the molecular sample through a copper coil. This results in the coupling between rotational states of ground-state molecules. Due to the low radiation efficiency of the coil, the maximum irradiation power of MW in the sample region is on the order of mW. In the following measurements, the irradiation power of MW is set at 100 μW.

As shown in Fig. 1(b), the loading procedure of dark-SPOTs and PA procedure are operated simultaneously, with a duration time of 90 ms, to produce molecules in the $X^1\Sigma^+$ (v = 0) state. Next, all the cooling lasers, PA laser and magnetic field are turned off. At the mean time, the MW field and depletion laser are switched on (2 ms) for the measurement of MW spectroscopy, or, for the depletion spectroscopy only the depletion laser is turned on (2 ms). Finally, the residual molecules are ionized through RETPI. The molecular ions are then accelerated by a pulsed electric field and detected by a pair of micro-channel plates (MCPs). After amplification, the electric signals can be monitored on a digital oscilloscope, and

Optics EXPRESS

recorded continuously using an NI PCI-1714 card with 10 averages following a boxcar (Boxcar, SRS-250). The repetition rate is 10 Hz in the experimental condition.

3. Experimental results and analysis

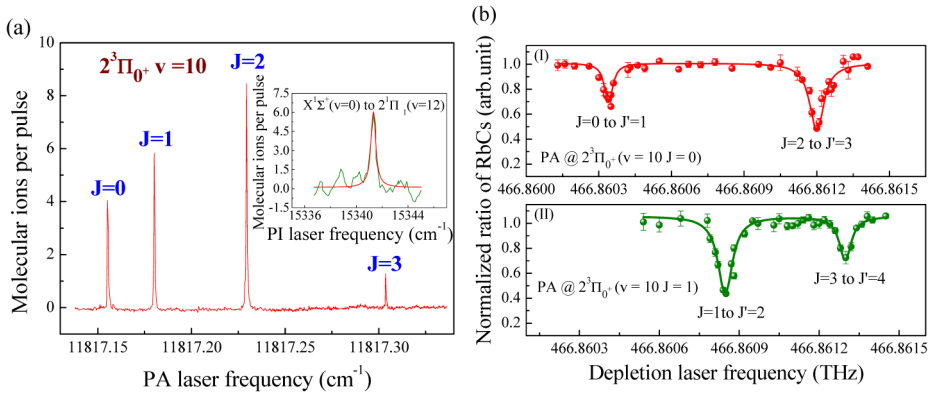

Fig. 2. (a) PA spectrum of $2^3\Pi_0$ + (v = 10) state, which is the intermediate state for the preparation of $^{85}Rb^{133}Cs$ molecules in the $X^1\Sigma^+$ (v = 0) state. Inset: PI spectrum of $^{85}Rb^{133}Cs$ molecules in the $X^1\Sigma^+$ (v = 0) state. (b) Depletion spectrum of molecules in the $X^1\Sigma^+$ (v = 0) state: (I) The frequency of PA laser is fixed at $2^3\Pi_0$ + (v = 10, J = 0), (II) The frequency of PA laser is fixed at $2^3\Pi_0$ + (v = 10, J = 1). The sum of depletion depths is over 90%, which indicates that the ion signal is produced through resonance excitation in our PI spectrum.

Figure 2(a) presents the rotational structure of the excited $2^3\Pi_0$ + (v = 10) state. Because this state has relatively large free-to-bound and bound-to-bound Frank-Condon factors (FCFs) [18], it can be used for the preparation of molecules in $X^1\Sigma^+$ (v = 0) state. In this work, the PA frequency is fixed at about 11817.16 cm $^{-1}$ (or 11817.18 cm $^{-1}$), corresponding to J = 0 (or J = 1) of $2^3\Pi_0$ + (v = 10) state. The PI spectrum has also been measured [see inset of Fig. 2(a)]. In the plots, the transition $X^1\Sigma^+$ (v = 0) → $2^1\Pi_1$ (v = 12) [24] has been taken.

In order to detect the rotational levels, the depletion spectrum of the $^{85}Rb^{133}Cs$ molecules in $X^1\Sigma^+$ (v = 0) state has been measured. The depletion laser frequency is scanned around the rotational levels between $X^1\Sigma^+$ (v = 0) and $2^3\Pi_0$ + (v = 8) states. Once the depletion laser is resonant with the transition, the distribution of the resonant rovibrational level in the $X^1\Sigma^+$ (v = 0) state can be depleted [see Fig. 2(b)]. In order to reduce the effect of drifts in the ion signal, we cycle the depletion laser on and off for consecutive detection pulses. The signals with and without the depletion laser are separately averaged after 200 cycles, and their ratio is calculated to obtain a normalized depletion signal. When the PA laser is locked to the $2^3\Pi_0$ + (v = 10, J = 0), the rotational population of $X^1\Sigma^+$ (v = 0) state is in the J = 0 and J = 2, whereas for the PA laser locked to the $2^3\Pi_0$ + (v = 10, J = 1), the rotational population of $X^1\Sigma^+$ (v = 0) is in the J = 1 and J = 3. Such rotational population of $X^1\Sigma^+$ (v = 0) is determined by the initial PA rotational level due to two-photon-cascade decay [22]. All the observed linewidth is about 80 MHz, which is broader than the natural linewidth of the excited state. Based on these measurements, the rotational levels could be detected selectively when the frequency of depletion laser is fixed at the resonant rovibrational transition. Furthermore, with the previous measured rotational spectra of $2^3\Pi_0$ + (v = 8) state [25], the rotational frequency spacing of $X^1\Sigma^+$ (v = 0) can be deduced as $\Delta\nu_{1\text{-}0} = f_1 + \Delta\nu'_{2\text{-}1} - f_2$, $\Delta\nu_{2\text{-}1} = f_2 + \Delta\nu'_{3\text{-}2} - f_3$ and $\Delta\nu_{3\text{-}2} = f_3 + \Delta\nu'_{4\text{-}3} - f_4$ [see the partial enlarged detail of Fig. 1(a)]. Here, the $\Delta\nu_{(J+1)\text{-}J}$ and $\Delta\nu'_{(J'+1)\text{-}J'}$ denote the frequency spacing of rotational levels of $X^1\Sigma^+$ (v = 0) and $2^3\Pi_0$ + (v = 8) states, respectively. In addition, f_i labels the frequency of transition $X^1\Sigma^+$ (v = 0, J)→$2^3\Pi_0$ + (v = 8,J' = J + 1).

Optics EXPRESS

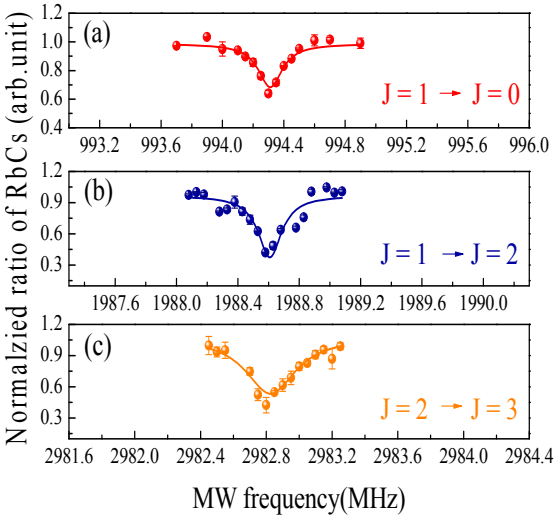

Fig. 3. MW spectrum of $^{85}Rb^{133}Cs$ molecules in the $X^1\Sigma^+$ (v = 0) state. (a) The MW transition of J = 1 → J = 0. The frequency of PA laser is fixed at $2^3\Pi_0$ + (v = 10, J = 1), the depletion laser is fixed at $X^1\Sigma^+$ (v = 0, J = 0) → $2^3\Pi_0$ + (v = 8, J' = 1). (b) The MW transition of J = 1 → J = 2. The frequency of PA laser is fixed at $2^3\Pi_0$ + (v = 10, J = 1), the depletion laser is fixed at $X^1\Sigma^+$ (v = 0, J = 2) → $2^3\Pi_0$ + (v = 8, J' = 3). (c) The MW transition of J = 2 → J = 3. The frequency of PA laser is fixed at $2^3\Pi_0$ + (v = 10, J = 0), the frequency of depletion laser is fixed at $X^1\Sigma^+$ (v = 0, J = 3) → $2^3\Pi_0$ + (v = 8, J' = 4).

Based on the short-range PA and depletion spectroscopy, we have experimentally determined three MW transitions in the $X^1\Sigma^+$ (v = 0) state by scanning the frequency of MW under different PA levels. In MW spectroscopy, rotational transitions between neighboring J states are allowed, so that the molecules in $X^1\Sigma^+$ (v = 0, J) level can be transferred to $X^1\Sigma^+$ (v = 0, J + 1) or $X^1\Sigma^+$ (v = 0, J - 1) level when applying a MW pulse. As mentioned before, the molecules in the J + 1 (or J-1) level could be detected selectively, provided the frequency of depletion laser is fixed at $X^1\Sigma^+$ (v = 0, J + 1) → $2^3\Pi_0$ + (v = 8, J' = J + 2) (or $X^1\Sigma^+$ (v = 0, J - 1) → $2^3\Pi_0$ + (v = 8, J' = J)). Figure 3 illustrates the typical spectrum of the MW transition. There, three rotational transitions based on MW spectroscopy in the $X^1\Sigma^+$ (v = 0) state are observed. The Fig. 3(a) shows the MW transition of J = 1 → J = 0 when the frequency of PA laser is fixed at $2^3\Pi_0$ + (v = 10, J = 1) and the depletion laser is fixed at $X^1\Sigma^+$ (v = 0, J = 0) → $2^3\Pi_0$ + (v = 8, J' = 1). The MW transition of J = 1 → J = 2 is presented in Fig. 3(b), while the frequency of PA laser is fixed at $2^3\Pi_0$ + (v = 10, J = 1) and the depletion laser is fixed at $X^1\Sigma^+$ (v = 0, J = 2) → $2^3\Pi_0$ + (v = 8, J' = 3). Figure 3(c) illustrates the MW transition J = 2 → J = 3, while the frequency of PA laser is fixed at $2^3\Pi_0$ + (v = 10, J = 0) and the frequency of depletion laser is fixed at $X^1\Sigma^+$ (v = 0, J = 3) → $2^3\Pi_0$ + (v = 8, J' = 4). The data point is averaged over 200 times. The FWHM of the resonance is measured to be around 200-300 kHz. According to [31], the hyperfine spacing of $^{85}Rb^{133}Cs$ molecules in the lowest vibrational state is on the order of 100 kHz. Even the electric and magnetic fields have been switched off during the measurement of depletion and microwave spectra, there are still stray magnetic fields arising mainly from the ion pump. However, the intensity of such field is small, which is measured to be less than 0.5 Gauss. This induces a Zeeman splitting on the order of 10 kHz following [31]. In addition, the temperature of the ultracold sample T is about 100 μK which, according to $k_B T/2 = h\nu$, indicates a thermal broadening ν of about 10 kHz. Here, k_B is Boltzmann constant and h is Planck constant. Thus, the measured linewidth of MW spectrum is mainly limited by the hyperfine spacing. In higher actual irradiation power

Optics EXPRESS

of MW (about 2 mW) or lower available depletion laser power (1mW), we haven't observed the frequency shift of the resonance center in the present experimental condition.

The deduced frequency spacing Δv with the depletion and MW spectroscopy allows us to obtain the rotational constant of molecular ground state. Figure 4(a) shows the dependence of Δv on the J for $^{85}Rb^{133}Cs$ in $X^1\Sigma^+$ (v = 0) state. The triangle dot represents the data obtained by the depletion spectroscopy, while the circle represents the data obtained by MW spectroscopy. For depletion spectroscopy, the Δv_{1-0}, Δv_{2-1}, Δv_{3-2} are found as 1020(13) MHz, 1945(16) MHz, and 2960(19) MHz, respectively. Here, the uncertainties are mainly caused by the measurement resolution of wavelength meter (~10 MHz), the uncertainty of locked depletion laser frequency (~2 MHz), the fitting error of the depletion spectroscopy (~1 MHz), and the uncertainty of the excited $2^3\Pi_0 + (v = 8)$ state rotational constant (~2 MHz). For MW spectroscopy, the Δv_{1-0}, Δv_{2-1}, Δv_{3-2} are deduced as 994.30(1) MHz, 1988.61(1) MHz, and 2982.82(1) MHz, respectively. The uncertainty mainly comes from the energy splitting due to stray magnetic fields (~10 kHz), thermal broadening (~10 kHz) and the fitting error of the MW spectroscopy (~2 kHz).

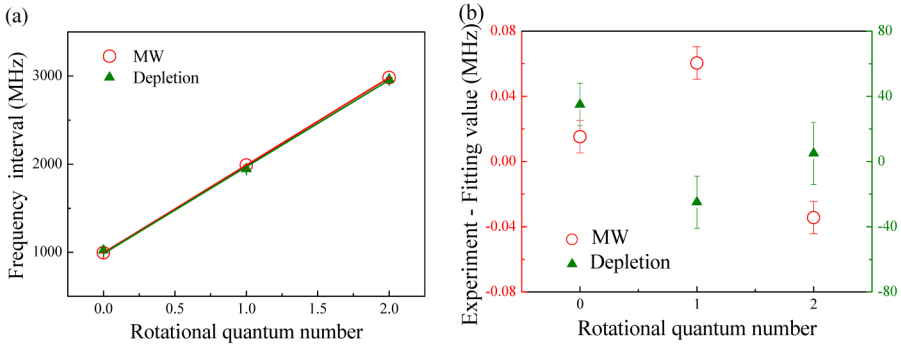

Fig. 4. (a) Dependence of the frequency spacing Δv on J for $^{85}Rb^{133}Cs$ in $X^1\Sigma^+$ (v = 0) state. The experimental data are deduced with the depletion and MW spectroscopy, while the lines are the fits to the rigid rotor model. (b) The difference of frequency spacing Δv between the fitting value and the experimental value.

The molecules in low vibrational states can be well described by the rigid rotor model [32]. Define the rotational frequency spacing by $\Delta v = 2B\ (J + 1)\ (J \geq 0)$, with B being the rotational constant. The solid lines are the fitting curves. The rotational constant obtained from the depletion spectroscopy is found as 493(4) MHz, where the uncertainty is the fitting error. This is consistent with the results obtained from the inverted perturbation approach which combines the laser-induced fluorescence and Fourier transform spectroscopy (497 MHz) [33], as well as that predicted from the density-functional theory (511 MHz) [31]. In contrast, the rotational constant obtained from MW spectroscopy is 497.14(1) MHz with the uncertainty being the fitting error, indicating a much higher accuracy is achieved compared to the depletion spectroscopy. The difference of Δv between the fitting value and the experimental value has also been derived for the depletion and MW spectroscopy, respectively. As illustrated by Fig. 4(b), we see that the measurement accuracy of MW spectroscopy increases by 3 orders of magnitude with respect to the depletion spectroscopy. We thus conclude that our MW spectroscopy is effective with higher accuracy in measuring the rotational structure of ground-state molecules.

4. Conclusion

We have obtained the high-resolution MW spectroscopy of ultracold $^{85}Rb^{133}Cs$ molecules in $X^1\Sigma^+$ (v = 0) ground state produced from short-range PA. With electric-dipole allowed transitions between the rotational levels, the MW field has been directly utilized to couple the

Optics EXPRESS

neighboring rotational levels. By scanning the MW frequency, the MW spectroscopy has been obtained by using the combination of CW depletion spectroscopy and PI technique. Using the rotational frequency spacing obtained from the MW spectroscopy, we have accurately determined the rotational constant of molecules in $X^1\Sigma^+$ (v = 0) state by fitting the frequency spacing to the rigid rotor model. Our experimental results by MW spectroscopy demonstrate a high precision, increasing by 3 orders of magnitude as compared to that from CW depletion spectroscopy. The present scheme provides a simple and high accuracy method for the measurement of molecular structures.

Funding

National Key Research and Development program (No. 2017YFA0304203); National Natural Science Foundation of China (NSFC) (Nos. 61675120, 11434007 and 61378015); NSFC Project for Excellent Research Team (No. 61121064); Shanxi Scholarship Council of China; "1331 KSC"; PCSIRT (No. IRT 13076); Applied Basic Research Project of Shanxi Province (No. 201601D202008).

218.26.34.65 {ts '2018-01-23 19:09:36'}